J. Fluid Mech. (1992), *vol.* 242, *pp.* 395–417
Printed in Great Britain

Instability of a solid-body rotating vortex in a two-layer model

By P. RIPA

Centro de Investigación Científica y de Educación Superior de Ensenada, 22800 Ensenada, Baja California, México

(Received 25 October 1991 and in revised form 10 February 1992)

The instability of an anticyclonic solid-body rotating eddy embedded on a quiescent environment is studied, for all possible values of the parameters of the unperturbed state, i.e. the vortex's relative thickness and rotation rate. The Coriolis force is fundamental for the existence of the eddy (because the pressure force has a centrifugal direction) and therefore this analysis pertains to the study of mesoscale vortices in the ocean or the atmosphere, as well as those in other planets.

These eddies are known to be stable when the 'second' layer is assumed imperturbable (infinitely deep); however, here these vortices are found to be unstable in the more realistic case of an active environment layer, which may be arbitrarily thick.

Three basic types of instability are found, classified according to the dynamic structure of the growing perturbation field, in both layers: *baroclinic instability* (Rossby-like in both layers), *Sakai instability* (Poincaré-like in the vortex layer and Rossby-like in the environment), and *Kelvin–Helmholtz instability* (Poincaré-like in both layers). In addition, there is a *hybrid instability*, which goes continuously from the baroclinic to the Sakai types, as the rotation rate is increased.

The problem is constrained by the conservation of pseudoenergy and angular pseudomomentum, which are quadratic (to lowest order) in the perturbation. The requirement that both integrals of motion vanish for a growing disturbance, determines the structure of the latter in both layers. Furthermore, that constraint restricts the region, in parameter space, where each type of instability is present.

1. Introduction

The study of the stability/instability of a given solution (the basic state) of a hydrodynamical model, is aided by the analysis of its conservation laws. If the basic flow is steady, then there is an integral of motion which is quadratic to lowest order in the perturbation: the pseudoenergy $\mathscr{I}_E$. The (angular) pseudomomentum $\mathscr{I}_M$ is similarly constructed for an (axial) symmetric basic state. An arbitrary combination of both integrals, say $\mathscr{I}_E - \alpha\mathscr{I}_M$, is used to analyse *a priori* the stability/instability properties of a basic flow, like the one studied here, which is both steady and symmetric.

The following is a sufficient stability condition:

$$\text{'}\exists\alpha \quad \text{such that } \mathscr{I}_E - \alpha\mathscr{I}_M \text{ is sign definite'}$$

and its contraposition is a necessary instability condition,

$$\text{'}\mathscr{I}_E - \alpha\mathscr{I}_M \text{ must be sign indefinite } \forall\alpha\text{'}$$

(see for instance Ripa 1991, hereinafter denoted by R91). The motion in phase space is constrained to the intersection of the family (with α as parameter) of hypersurfaces $\mathscr{I}_E - \alpha \mathscr{I}_M =$ constant. If the basic state is unstable, then there are trajectories that leave any neighbourhood – no matter how small – of this point of phase space. Since that neighbourhood may be arbitrarily small, the family of hypersurfaces $\mathscr{I}_E - \alpha \mathscr{I}_M = 0$ go through the basic state point,† defining the stable and unstable manifolds; this property is used in the following section to discuss *a priori* the properties of growing and decaying perturbations.

As an example, consider a perturbation composed of just one growing or decaying normal mode, i.e. a solution of the linearized equations with an $\exp(-i\omega t + \lambda t)$ time dependence, such that ω and λ are real, and λ is either positive or negative: Since the quadratic part of $\mathscr{I}_E$ and $\mathscr{I}_M$ is both constant and proportional to $\exp(2\lambda t)$, it must be $\mathscr{I}_E = \mathscr{I}_M = 0$ for this particular perturbation; a similar argument holds for an algebraically growing disturbance. Now, a vanishing value of both $\mathscr{I}_E$ and $\mathscr{I}_M$ is accomplished through a compensation of its positive and negative parts: this balance might say something on the nature of a growing perturbation.

Ocean anticyclones are often studied with the so-called $1\frac{1}{2}$-layer (or one-layer reduced gravity) model; if the vortex is solid-body rotating and circular, then it is not only normal modes stable (Killworth 1983) but also formally stable (Ripa 1987, hereinafter referred to as R87), i.e. stable to perturbations of arbitrary shape, in the sense described above ($\mathscr{I}_E - \alpha \mathscr{I}_M$ positive definite, for some α and any perturbation). (As a remainder of the difference between both kinds of stability, recall that Couette flow is (formally) unstable to perturbations which grow linearly with time, even though it is stable to normal mode perturbations.) However, a sufficiently elliptical vortex (in the same $1\frac{1}{2}$-layer model) becomes unstable (R87; Ripa & Jiménez 1988). In this paper I investigate the possibility of another destabilizing agent: an active second layer; Paldor & Nof (1990) have studied the instability of a particular subset of the vortices considered here, namely those with vanishing potential vorticity.

A vortex which is stable in the $1\frac{1}{2}$-layer model may become unstable in a two-layer system, for two reasons: it is harder to guarantee positive definiteness of wave energy (R91), and there are more degrees of freedom available to construct a growing disturbance. The latter is seen clearly if the perturbation is Galerkin expanded, as done here, following Sakai (1989). Although both the $1\frac{1}{2}$- and 2-layer systems are mathematically well-posed problems, it is obvious that the latter allows for a more realistic approximation to real ocean dynamics. The importance of the second layer has been pointed out by other authors, in different scenarios (e.g. Chassignet & Cushman-Roisin 1991); one common objective to all these studies is to determine to what extent, and when, is the $1\frac{1}{2}$-model a good approximation of the more realistic 2-layer one.

The rest of this paper is organized as follows: the model equations, conservation laws, and their implications for the stability problem are discussed in §2. The following section is devoted to the development of the Galerkin basis for the variables in each layer (some mathematical details are left for an Appendix). A complete description of the stability analysis is given in §4, and the general conclusions are presented in the last section.

† If the system is formally stable, on the other hand, for those values of α such that the first theorem applies, the set for $\mathscr{I}_E - \alpha \mathscr{I}_M = 0$ is just the basic state point.

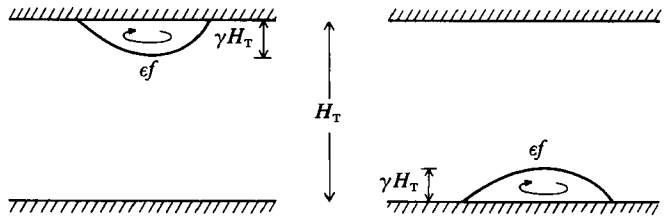

FIGURE 1. Cross-section of the basic state: a vortex is solid-body rotating at an (anticyclonic) angular speed $-\epsilon f$ ($0 < \epsilon < 1$), and its maximum thickness equals γ times the total depth of the system ($0 < \gamma < 1$).

2. Model equations

Consider an anticyclonic eddy, solid body rotating at an angular speed σ and with radius a (see figure 1); $\sigma = \Omega + \Omega_*$ of the limiting case of a circular vortex in R87. Let the vortex fluid, denoted by a subscript v, be immersed in another layer (subscript e, for environment) whose horizontal extent is the whole f-plane. The thicknesses H, and the radial U and azimuthal V velocity components in this basic state are given by

$$[g_r H_v, U_v, V_v] = [\tfrac{1}{2}\sigma(f-\sigma)(a^2-r^2), 0, -\sigma r] \quad (0 \leqslant r \leqslant a),$$

in the vortex layer, and

$$[g_r H_e, U_e], V_e = \begin{cases} [g_r H_T - g_r H_v, 0, 0] & (0 \leqslant r \leqslant a), \\ [g_r H_T, 0, 0] & (a \leqslant r), \end{cases}$$

in the environment layer, where the three constants g_r, f and H_T are the buoyancy jump across the interface between both layers, Coriolis parameter, and total depth of the model, respectively. Notice that uniform rotation corresponds to a parabolic profile of the interface. The potential vorticity fields in this basic state are given by

$$Q_v(r) = (f-2\sigma)/H_v(r), \quad Q_e(r) = f/H_e(r).$$

Two non-dimensional parameters characterize any one of these equilibrium states: the Rossby number and the relative vortex depth

$$\epsilon := \sigma/f, \quad \gamma := H_v(0)/H_T;$$

here I am interested in the range $0 < \epsilon < 1$, $0 < \gamma < 1$, which corresponds to the physically meaningful solutions (except that γ could be larger than unity, indicating a vortex that covers the whole vertical extent of the model, with fronts in both horizontal boundaries). The interpretation of these parameters follows.

The radial momentum equation inside the basic vortex shows that the Coriolis acceleration $-fV_v$ equals the sum of the pressure force $-g_r\,\mathrm{d}H_v/\mathrm{d}r$ plus the centrifugal force V_v^2/r; the last two terms have the same sign, and each one becomes negligible – with respect to the other one – in the limits $\epsilon \to 1$ and $\epsilon \to 0$, respectively. At $\epsilon = \frac{1}{2}$, pressure and centrifugal force are identical and the potential vorticity in the vortex layer vanishes; this is the case studied by Paldor & Nof (1990).

On the other hand, $\gamma = 0$ corresponds to the $1\frac{1}{2}$-layer model ($H_T \to \infty$), in which the vortex is formally stable, as discussed in §1 (this includes the range $\epsilon > \frac{1}{2}$, where the necessary, but not sufficient, condition for inertial stability is satisfied). Finally, for $\gamma \to 1$, the vortex 'kisses' the opposite horizontal boundary.

Let φ_v and φ_e denote the perturbation fields in both layers, $\varphi := (p, \boldsymbol{u})$ with $\boldsymbol{u} := (u, v)$. The linearized evolution equations can be written in the form

$$\partial_t \varphi_v + \mathbb{L}_v \varphi_v = (\partial_t + \boldsymbol{U}_v \cdot \boldsymbol{\nabla})\, \mathbb{P}\varphi_e,$$
$$\partial_t\, \mathbb{D}\varphi_e + \mathbb{L}_e \varphi_e = \partial_t\, \mathbb{D}\mathbb{P}\varphi_v,$$

where $\mathbb{L}$, $\mathbb{P}$ and $\mathbb{D}$ are 3×3 matrix operators, defined by

$$\mathbb{L}_v := \begin{pmatrix} \boldsymbol{U}_v\cdot\boldsymbol{\nabla} & g_r \partial_x(H_v & g_r \partial_y(H_v \\ \partial_x & \boldsymbol{U}_v\cdot\boldsymbol{\nabla} & -f_* \\ \partial_y & f_* & \boldsymbol{U}_v\cdot\boldsymbol{\nabla} \end{pmatrix},$$

$$\mathbb{L}_e := \begin{pmatrix} 0 & g_r \partial_x(H_v & g_r \partial_y(H_v \\ \partial_x & 0 & -f \\ \partial_y & f & 0 \end{pmatrix},$$

$$\mathbb{P} = \begin{pmatrix} 1 & 0 & 0 \\ 0 & 0 & 0 \\ 0 & 0 & 0 \end{pmatrix}, \quad \mathbb{D} := \begin{pmatrix} 1 & 0 & 0 \\ 0 & 1 & 0 \\ 0 & 0 & 1 \end{pmatrix} \ (r < a) \quad \text{or} \quad \mathbb{D} := \begin{pmatrix} 0 & 0 & 0 \\ 0 & 1 & 0 \\ 0 & 0 & 1 \end{pmatrix} \ (r > a),$$

with $f_* := f - 2\sigma$. The effect of the basic state is a non-uniform topography for both layers; in addition, the first layer suffers an advection and a change of the effective Coriolis parameter. The coupling of the state variables of both layers is done through the interface elevation ζ (the perturbed depth of each layer equals $H_v - \zeta$ and $H_e + \zeta$, respectively), which satisfies $p_e - p_v = g_r \zeta$.

The linearized laws of potential vorticity conservation are

$$(\partial_t + \boldsymbol{U}_v \cdot \boldsymbol{\nabla})\, \xi_v + u_v Q_{v,r} = 0, \quad \partial_t \xi_e + u_e Q_{e,r} = 0,$$

where $$\xi_v := (\hat{\boldsymbol{z}} \cdot \boldsymbol{\nabla} \times \boldsymbol{u}_v + \zeta Q_v)/H_v, \quad \xi_e := (\hat{\boldsymbol{z}} \cdot \boldsymbol{\nabla} \times \boldsymbol{u}_e - \zeta Q_e)/H_e$$

are the first variations of potential vorticity, $Q_{v,r} := \mathrm{d}Q_v/\mathrm{d}r\,(= r\sigma(f-\sigma)\,(f-2\sigma)\,H_v^{-2}$ in our case) and $Q_{e,r} := \mathrm{d}Q_e/\mathrm{d}r = -r\sigma(f-\sigma)f H_e^{-2}$.

Two quadratic integrals of motion are derived from the linearized evolution equations for the perturbation: the pseudoenergy $\mathscr{I}_E$, which owes its existence to time-invariance of both the model equations and the basic flow, and the (angular) pseudomomentum $\mathscr{I}_M$, derived from the axisymmetry of model equations and basic state. The pseudoenergy is the sum of the wave energy and a Casimir, say, $\mathscr{I}_E = \mathscr{E} + \mathscr{C}_E$; similarly the pseudomomentum is the sum of the wave angular momentum and another Casimir, $\mathscr{I}_M = \mathscr{M} + \mathscr{C}_M$. The Casimirs are just functionals of the potential vorticity perturbation field, suitably chosen so that $\mathscr{I}_E$ = constant and $\mathscr{I}_M$ = constant (see R91). It is important to point out that $\mathscr{I}_E$ and $\mathscr{I}_M$ are the lowest-order (quadratic) term of two exact integrals of motion, of the fully nonlinear problem (R91).

As mentioned before $\mathscr{E}$ is the wave energy, and $\mathscr{M}$ is the wave momentum, measured in the f-plane: it is easy to see that $\mathscr{E} - \alpha\mathscr{M}$ equals the wave energy in a frame rotating with speed α relative to the earth. [This should not be taken as implying that the evolution equations are covariant under a change to a rotating frame; the are not (see R87).] In order to present the formulae for $\mathscr{I}_E$ and $\mathscr{I}_M$, it is useful to split a general combination of both integrals of motion in the form

$$\mathscr{I}_E - \alpha\mathscr{I}_M = \underbrace{\mathscr{E}_v^k(\alpha) + \mathscr{E}_e^k(\alpha) + \mathscr{E}^p}_{\mathscr{E} - \alpha\mathscr{M}} + \underbrace{\mathscr{C}_v(\alpha) + \mathscr{C}_e(\alpha)}_{\mathscr{C}_E - \alpha\mathscr{C}_M},$$

Contribution	Condition for positive definiteness
$\mathscr{E}_{\mathrm{v}}^{\mathrm{k}}(\alpha)+\mathscr{E}_{\mathrm{e}}^{\mathrm{k}}(\alpha)+\mathscr{E}^{\mathrm{p}}$	$\alpha/\sigma=-1,\ 2\gamma\epsilon<1-\epsilon$
$\mathscr{C}_{\mathrm{v}}(\alpha)$	$(\alpha/\sigma+1)(2\epsilon-1)>0$
$\mathscr{C}_{\mathrm{e}}(\alpha)$	$\alpha/\sigma>0$

TABLE 1

where $\mathscr{E}_{\mathrm{v}}^{\mathrm{k}}(\alpha)$ and $\mathscr{E}_{\mathrm{e}}^{\mathrm{k}}(\alpha)$ are the kinetic and $\mathscr{E}^{\mathrm{p}}$ is the potential wave energies. The individual contributions (multiplied by $2g_{\mathrm{r}}$, for simplicity) are

$$\mathscr{E}_{\mathrm{v}}^{\mathrm{k}}(\alpha) := \int_{r<a} \mathrm{d}^2x\,[g_{\mathrm{r}} H_{\mathrm{v}} \boldsymbol{u}_{\mathrm{v}}^2 + 2(V_{\mathrm{v}}-\alpha r)\, v_{\mathrm{v}}(p_{\mathrm{v}}-p_{\mathrm{e}})],$$

$$\mathscr{E}_{\mathrm{e}}^{\mathrm{k}}(\alpha) := \int_{r<\infty} \mathrm{d}^2x\, g_{\mathrm{r}} H_{\mathrm{e}} \boldsymbol{u}_{\mathrm{e}}^2 + 2\int_{r<a} \mathrm{d}^2x\, \alpha r v_{\mathrm{e}}(p_{\mathrm{v}}-p_{\mathrm{e}}),$$

$$\mathscr{E}^{\mathrm{p}} := \int_{r<a} \mathrm{d}^2x\,(p_{\mathrm{v}}-p_{\mathrm{e}})^2,$$

$$\mathscr{C}_{\mathrm{v}}(\alpha) := \int_{r<a} \mathrm{d}^2x\, g_{\mathrm{r}} H_{\mathrm{v}}^2 \frac{V_{\mathrm{v}}-\alpha r}{Q_{\mathrm{v,r}}} \xi_{\mathrm{v}}^2,$$

$$\mathscr{C}_{\mathrm{e}}(\alpha) := -\int_{r<a} \mathrm{d}^2x\, g_{\mathrm{r}} H_{\mathrm{e}}^2 \frac{\alpha r}{Q_{\mathrm{e,r}}} \xi_{\mathrm{e}}^2.$$

The sum of the five terms above is then an integral of motion for an arbitrary initial perturbation and for any value of α. Our next task is to discuss the relative importance of the various terms, and relate it to the nature of particular perturbations in each layer. In particular, one wants to compare the positive definite terms with those that might be negative (second part of the wave kinetic energies and wave Casimirs) because for a perturbation growing away from an unstable basic state it must be possible to get $\mathscr{I}_{\mathrm{E}}-\alpha\mathscr{I}_{\mathrm{M}}=0\forall\alpha$, as discussed in §1.

Table 1 shows in which region of parameter space (ϵ, γ), and for which values of α, each one of three contributions to $\mathscr{I}_{\mathrm{E}}-\alpha\mathscr{I}_{\mathrm{M}}$ (wave energy and wave Casimir in each layer) is positive definite. For instance, in order for the wave energy to be positive definite, it is necessary that $(V_{\mathrm{v}}-\alpha r)^2/H_{\mathrm{v}}+(\alpha r)^2/H_{\mathrm{e}}<g_{\mathrm{r}}$, $\forall r$ (R91); since $H_{\mathrm{v}}=0$ at $r=a$, this condition can only be satisfied for $\alpha=V_{\mathrm{v}}(a)/a=-\sigma$, and it further requires $2\gamma\epsilon<1-\epsilon$. The other two conditions come from the analysis of the sign of $(V-\sigma r)\,\mathrm{d}Q/\mathrm{d}r$, in each layer.

Primitive equations models have, usually, two types of waves: Poincaré and Rossby ones. Poincaré waves are mainly due to gravity effects, and are affected by earth's rotation. Rossby waves, on the other hand, owe their existence to a gradient of ambient potential vorticity, either because of the change of the Coriolis parameter with latitude (planetary modes) and/or to inhomogeneities in the thickness of an isopycnal layer (topographic modes).

Poincaré waves have a negligible potential vorticity perturbation and an important horizontal divergence, namely $H^2|\xi| \ll |\nabla\cdot(H\boldsymbol{u})|$; for these modes it is $|\mathscr{E}-\alpha\mathscr{M}| \gg |\mathscr{C}_{\mathrm{E}}-\alpha\mathscr{C}_{\mathrm{M}}|$ (except for very large horizontal scales, compared with the deformation radius, i.e. in the limit of inertial waves, in which both parts of the integrals of motion are of the same order), simply because the Casimirs are functionals of ξ^2. The opposite is true for Rossby waves: Indeed, in the quasi-

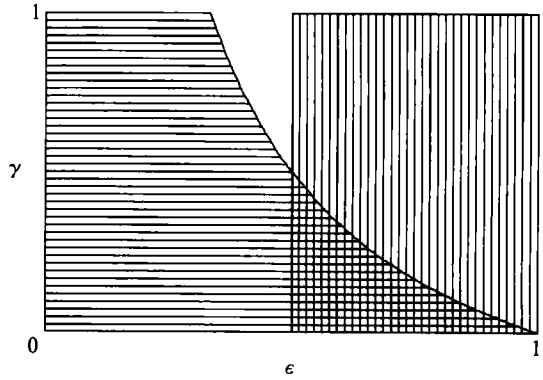

FIGURE 2. *A priori* predictions from pseudoenergy and angular pseudomomentum conservation: for unstable vortices in the horizontally (vertically) hatched region, a growing perturbation must be Rossby-like in the environment layer (Poincaré-like in the vortex layer).

geostrophic theory (which filters out Poincaré modes) the horizontal flow and the wave energy are *a priori* assumed to be exactly non-divergent and positive definite, respectively (e.g. see Ripa 1992).

The following general conclusions can be obtained, from analysis of table 1:

(*a*) There is no value of α such that $\mathscr{I}_{\mathrm{E}}-\alpha\mathscr{I}_{\mathrm{M}}$ is sign definite, for any vortex (i.e. for any value of γ and ϵ); therefore, no vortex in this family is formally stable (i.e. if there are stable vortices, their stability cannot be proved by Arnol'd's method).

(*b*) If $\epsilon > \frac{1}{2}$ (vertically hatched region in figure 2), the only non-positive definite contribution to the pseudoenergy in the Earth's frame, $\mathscr{I}_{\mathrm{E}}$, comes from $\mathscr{E}^{\mathrm{k}}_{\mathrm{v}}(0)$. Consequently, for unstable vortices in this region of parameter space, a growing perturbation must have a Poincaré-like structure in the vortex layer. This component must have a negative kinetic wave energy, large enough to balance all other terms (which are positive).

(*c*) If $3\epsilon < 1$ or $[3\epsilon > 1$ and $2\gamma\epsilon < 1-\epsilon]$ (horizontally hatched region in figure 2), on the other hand, the only non-positive definite contribution to the pseudoenergy in a frame rotating with the vortex, $\mathscr{I}_{\mathrm{E}}+\sigma\mathscr{I}_{\mathrm{M}}$, comes from $\mathscr{C}_{\mathrm{e}}(-\sigma)$. Consequently, for unstable vortices in this region of parameter space, a growing perturbation must have a Rossby-like structure in the environment layer. The potential vorticity disturbance must be large enough for the wave Casimir in this layer to balance all other terms, which are positive definite.

One system where the statement $|\mathscr{M}| \gg |\mathscr{C}_{\mathrm{M}}|$ ($|\mathscr{M}| \ll |\mathscr{C}_{\mathrm{M}}|$) for Poincaré (Rossby) waves has been shown explicitly is the equatorial β-plane (Ripa 1982); this system also has a mode that goes continuously from being Poincaré-like to being Rossby-like – the Yanai wave. We shall find that also in the problem studied here, and therefore predictions (*b*) and (*c*) (conjectured in R91) will need some qualification.

The integrals of motion were deduced making no assumption on the structure of the perturbation (in fact, they are written so that they are correct for profiles V_{v} not necessarily equal to $-\sigma r$). Takehiro & Hayashi (1992) have shown how the stability/instability results derived from conservation laws are related to the concepts of over-reflection and turning and critical lines. This section finishes with a heuristic interpretation of both regions in figure 2. In the first place, if $\epsilon < \frac{1}{2}(\epsilon > \frac{1}{2})$, the gradient of ambient potential vorticity in the vortex layer is towards (away from) the centre; the basic flow is 'westward' ('eastward'). Consequently, for vortices in the vertically hatched region of figure 2 there cannot exist Rossby waves (say, in a

WKB sense) in the vortex layer with a critical radius (consistent with point (*b*) above). On the other hand, it is possible to show that for vortices in the horizontally hatched region it is $g_r H_e(r) > V_v^2(r)$ $(0 < r < a)$, i.e. the Poincaré waves in the environment layer travel faster than the vortex and are effectively decoupled from a perturbation with a critical radius there (consistent with point (*c*) above). These heuristic arguments also apply to the analysis of the following section, in which the perturbation is Galerkin expanded in the manner of Sakai (1989).

3. Expansion of the perturbation

The operators $-\mathrm{i}\mathbb{L}_v$ and $-\mathrm{i}\mathbb{L}_e$ are self-adjoint, in the sense of scalar products

$$\langle \hat{\phi}_a, \hat{\phi}_{a'} \rangle := \int_{r<a} \mathrm{d}^2x \, (g_r H_v \hat{\boldsymbol{u}}_a^* \cdot \hat{\boldsymbol{u}}_{a'} + \hat{p}_a^* \hat{p}_{a'}),$$

$$[\tilde{\phi}_b, \tilde{\phi}_{b'}] := \int \mathrm{d}^2x \, g_r H_e \tilde{\boldsymbol{u}}_b^* \cdot \tilde{\boldsymbol{u}}_{b'} + \int_{r<a} \mathrm{d}^2x \, \tilde{p}_b^* \tilde{p}_{b'},$$

where the * denotes complex conjugate. That means that the eigensolutions of $-\mathrm{i}\mathbb{L}_v \hat{\phi}_a = \hat{\omega}_a \hat{\phi}_a$ and $-\mathrm{i}\mathbb{L}_e \tilde{\phi}_b = \tilde{\omega}_b \mathbb{D} \tilde{\phi}_b$ have real eigenvalues, $\hat{\omega}_a$ and $\tilde{\omega}_b$, and orthogonal eigenvectors. Furthermore the latter form a complete basis, $\{\hat{\phi}_a\} \cup \{\tilde{\phi}_b\}$, suitable for the expansion of the perturbation fields, say

$$\varphi_v(\boldsymbol{x}, t) = \sum_a A_a(t) \hat{\phi}_a(\boldsymbol{x}), \quad \varphi_e(\boldsymbol{x}, t) = \sum_b B_b(t) \tilde{\phi}_b(\boldsymbol{x}).$$

The eigenvectors are normalized so that

$$\langle \hat{\phi}_a, \hat{\phi}_{a'} \rangle = \delta_{aa'}, \quad [\tilde{\phi}_b, \tilde{\phi}_{b'}] = \delta_{bb'},$$

from which it follows $A_a = \langle \hat{\phi}_a, \varphi_v \rangle$ and $B_b = [\tilde{\phi}_b, \varphi_e]$.

Notice that $\langle \varphi_v, \varphi_v \rangle$ is but the contribution of φ_v to $\mathscr{I}_E + \sigma \mathscr{I}_M$ (which is the pseudoenergy in a frame rotating with the vortex), whereas $[\varphi_e, \varphi_e]$ is the contribution of φ_e to $\mathscr{I}_E$ (in the earth's frame). It is easy to show that the contribution of φ_v to both $\mathscr{I}_E$ and $\mathscr{I}_M$ has a diagonal representation in $\{\hat{\phi}_a\}$, and similarly for φ_e and $\{\tilde{\phi}_b\}$. In order to do that, first the axisymmetry of the problem is used to make $\hat{\phi}_a$, $\tilde{\phi}_b \propto \exp(\mathrm{i}m\vartheta)$, where ϑ is the polar angle and m is the corresponding wavenumber. It then follows from $-\mathrm{i}\mathbb{L}_v \hat{\phi}_a = \hat{\omega}_a \hat{\phi}_a$ and $-\mathrm{i}\mathbb{L}_e \tilde{\phi}_b = \tilde{\omega}_b \mathbb{D} \tilde{\phi}_b$ and the normalization of the eigenvectors that

$$\int_{r<a} \mathrm{d}^2x \left(r \hat{v}_a^* \hat{p}_{a'} + g_r H_v^2 \frac{r}{Q_{v,r}} \hat{\xi}_a^* \hat{\xi}_{a'} \right) = \frac{m}{\hat{\omega}_a + m\sigma} \delta_{aa'},$$

$$\int_{r<a} \mathrm{d}^2x \left(r \tilde{v}_b^* \tilde{p}_{b'} + g_r H_e^2 \frac{r}{Q_{e,r}} \tilde{\xi}_b^* \tilde{\xi}_{B'} \right) = \frac{m}{\tilde{\omega}_b} \delta_{bb'}.$$

With these results it is trivial to derive the diagonal terms in the expansion of both $\mathscr{I}_E$ and $\mathscr{I}_M$, namely,

$$\mathscr{I}_E = \sum_a \frac{\hat{\omega}_a}{\hat{\omega}_a + m\sigma} |A_a(t)|^2 + \sum_b |B_b(t)|^2 + \mathrm{Re} \sum_{ab} \ldots A_a^*(t) B_b(t) = \text{constant},$$

for the pseudoenergy, and

$$\mathscr{I}_M = \sum_a \frac{m}{\hat{\omega}_a + m\sigma} |A_a(t)|^2 + \sum_b \frac{m}{\tilde{\omega}_b} |B_b(t)|^2 + \mathrm{Re} \sum_{ab} \ldots A_a^*(t) B_b(t) = \text{constant},$$

for the angular pseudomomentum. There are, of course, non-diagonal terms, which come from the integral of $-2(V_v v_v p_e + p_v p_e)$, for $\mathscr{I}_E$, or the integral of $-2r(v_v p_e + v_e p_v)$, for $\mathscr{I}_M$; the explicit form of the coefficients for these crossed terms, indicated by '...', is not important here.

I will now derive the equations for the normal modes, and show its relationship with these two conservation laws. Using the expansions $\varphi_v = \Sigma A_a \hat{\phi}_a$ and $\varphi_e = \Sigma B_b \tilde{\phi}_b$ and the orthogonality conditions $\langle \hat{\phi}_a, \hat{\phi}_{a'} \rangle = \delta_{aa'}$ and $[\tilde{\phi}_b, \tilde{\phi}_{b'}] = \delta_{bb'}$ in the evolution equations $\partial_t \varphi_v + \mathbb{L}_v \varphi_v = (\partial_t + \boldsymbol{U}_v \cdot \boldsymbol{\nabla}) \mathbb{P} \varphi_e$ and $\mathbb{D} \partial_t \varphi_e + \mathbb{L}_e \varphi_e = \mathbb{D} \mathbb{P} \partial_t \varphi_v$, and assuming an $\exp(-i\omega t)$ time dependence, it is easily obtained

$$(\hat{\omega}_a - \omega) A_a + (\omega + m\sigma) \sum_b{}' \mu_{ab} B_b = 0,$$

$$(\tilde{\omega}_b - \omega) B_b + \omega \sum_a{}' \mu_{ab} A_a = 0,$$

where the prime indicates sum over components with same azimuthal wavenumber m, and

$$\mu_{ab} := \int_{r<a} \mathrm{d}^2 x \, \hat{p}_a^* \tilde{p}_b.$$

Recalling the normalization $\langle \hat{\phi}_a, \hat{\phi}_a \rangle = [\tilde{\phi}_b, \tilde{\phi}_b] = 1$, it follows that $|\mu_{ab}| < 1$; the $\hat{\phi}_a$ and $\tilde{\phi}_b$ are normalized so that $\hat{p}_a$ and $\tilde{p}_b$ are real – apart from the factor $\exp(im\vartheta)$ – and so is μ_{ab}. Consequently the normal modes equations are of the form

$$\mathbb{J} \chi = \omega \mathbb{K} \chi,$$

where χ groups the A_a and B_b terms, and $\mathbb{J}$ and $\mathbb{K}$ are (infinite dimensional) real matrices. $\mathbb{K}$ is symmetric, but $\mathbb{J}$ is non-symmetric (if $m \neq 0$) on account of the term $m\sigma$. For $m = 0$ both matrices are hermitian and therefore the ω are real: there is no symmetric, or inertial, instability in this problem, even though for $\epsilon > \frac{1}{2}$ it is $fQ < 0$ in the vortex layer.

In order to avoid confusion, I will use the word 'modes' for the eigensolutions of the coupled system, i.e. the solutions of the physical problem, whereas the word 'component' will be used for the elements of either basis, used in the expansion. The latter are much easier to calculate than the former, because they come from a self-adjoint problem, and with less variables. The normal modes are then obtained as the eigenvectors of $\mathbb{K}^{-1}\mathbb{J}$; this is done (in §4) for a suitably chosen subset of the basis $\{\hat{\phi}_a\} \cup \{\tilde{\phi}_b\}$. Of course, it is a delicate question to decide which components to include in the calculation, for a given pair (ϵ, γ).

In order to gain insight into which components might produce an instability ($\mathrm{Im}(\omega) \neq 0$), following Sakai (1989) I will start by analysing the simplest non-trivial case: only two components, one from each layer. Making the 2×2 determinant equal to zero it is easily obtained (omitting subscripts for simplicity)

$$\begin{aligned}
[2\omega(1-\mu^2) - \hat{\omega} - \tilde{\omega} - \mu^2 m\sigma]^2 &= (\hat{\omega} + \tilde{\omega} + \mu^2 m\sigma)^2 - 4(1-\mu^2)\hat{\omega}\tilde{\omega} \\
&\equiv (\hat{\omega} + \tilde{\omega} + \mu^2 m\sigma)^2 + 4\mu^2(\tilde{\omega} + m\sigma)\hat{\omega} \\
&\equiv (\hat{\omega} + \tilde{\omega} + \mu^2 m\sigma)^2 + 4\mu^2(\hat{\omega} + m\sigma)\tilde{\omega};
\end{aligned}$$

in order to be $\mathrm{Im}(\omega) \neq 0$, it must be

$$(\hat{\omega} + m\sigma)\hat{\omega} < 0, \quad (\tilde{\omega} + m\sigma)\tilde{\omega} < 0,$$

i.e. both $\hat{\omega}$ and $\tilde{\omega}$ must be between 0 and $-m\sigma$. (Notice that this is necessary, but not

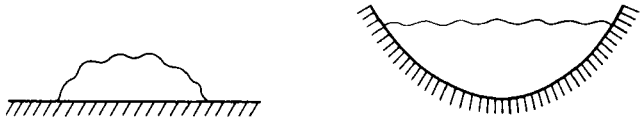

FIGURE 3. Equivalent physical system (cross-section) for the evaluation of the expansion components for the vortex layer: an anticyclonic eddy in a one-layer model or Laplace tidal equations on a revolution paraboloid.

sufficient, for instability; for instance if $\hat{\omega} = \tilde{\omega}$, for $\mathrm{Im}(\omega) \neq 0$ it is further needed that $(\mu m\sigma)^2 < -4(\hat{\omega}+m\sigma)\hat{\omega}$.) Let me point out the relationship of this result with the sign-definiteness of the integrals of motion $\mathscr{I}_{\mathrm{E}}$ and $\mathscr{I}_{\mathrm{M}}$:

The general combination $\mathscr{S}(\alpha) := \mathscr{I}_{\mathrm{M}} - \alpha\mathscr{I}_{\mathrm{M}}$, when evaluated at the two-component truncation, takes the form $\mathscr{S}(\alpha) = S_{11}|A|^2 + S_{22}|B|^2 + 2S_{12}\,\mathrm{Re}\,(A^*B)$, with $S_{11}S_{22} \equiv (\hat{\omega}-m\alpha)(\tilde{\omega}-m\alpha)/\tilde{\omega}(\hat{\omega}+m\sigma)$. If the basic state is unstable for some perturbation expanded by these two components, then all $\mathscr{S}(\alpha)$ must be sign indefinite, i.e. $S_{11}S_{22} < S_{12}^2\ \forall\,\alpha$. Now, $(\hat{\omega}+m\sigma)\,\hat{\omega} < 0$ implies that $S_{11}S_{22} < 0 (\leqslant S_{12}^2)$ for $\alpha = 0$, and therefore $\mathscr{S}(0)$ $(\equiv \mathscr{I}_{\mathrm{E}})$ is sign indefinite; similarly $(\tilde{\omega}+m\sigma)\,\tilde{\omega} < 0$ implies likewise for $\mathscr{S}(-\sigma)$, and $(\hat{\omega}+m\sigma)\tilde{\omega} < 0$ for $\mathscr{S}(\pm\infty)$ $(\propto \mathscr{I}_{\mathrm{M}})$. Moreover, if $\hat{\omega} \equiv \tilde{\omega}$, then $\mathscr{S}$ is sign indefinite for all α, which is the necessary condition for instability. The condition $\hat{\omega} = \tilde{\omega}$ defines a curve in the (ϵ, γ) space; it is expected (and will be shown) that the instability region will cover a finite area in that space, but its extent cannot be determined *a priori*, without explicit knowledge of the value of S_{12}.

Sakai (1989) argues, in a similar problem, that the instability region will be near the points where $\hat{\omega} = \tilde{\omega}$, and he calls this a *resonance* between both components. I have a semantic objection to the use of the word 'resonance' in this context, which I shall discuss later. Nevertheless, I am following closely Sakai's intuition in constructing both bases and looking for pairs of components such that $\hat{\omega} \approx \tilde{\omega}$ in the region where $(\hat{\omega}+m\sigma)\,\hat{\omega} < 0$; afterwards the calculation is refined adding more components, similar to those two.

Since this paper is to a great extent based in that of Sakai, it might be interesting to point out a couple of small differences between the works. First, I use both pseudoenergy and pseudomomentum (rather than just the latter), which gives the full scenario of figure 2 and the conclusions above (with pseudomomentum alone, only $(\hat{\omega}+m\sigma)\,\tilde{\omega} < 0$ is obtained). Secondly, there is the distinction between pseudoenergy and disturbance energy (or momenta): the latter is the sum of the wave energy $\mathscr{E}$ plus the mean flow energy, say $\mathscr{E}^0$. It is not possible to calculate $\mathscr{E}^0$ with the solution of the linearized equations (i.e. with φ_{v} and φ_{e}), however, its rate of change equals that of the Casimir $\mathscr{C}_{\mathrm{E}}$; consequently, when evaluated at a growing perturbation $\mathscr{E}^0$ and $\mathscr{C}_{\mathrm{E}}$ coincide, and so do pseudoenergy and disturbance energy. However, if evaluated at a neutral normal mode (or for a general perturbation), it is $\mathscr{E}^0 \not\equiv \mathscr{C}_{\mathrm{E}}$; pseudoenergy $\mathscr{E}+\mathscr{C}_{\mathrm{E}}$ (which is a more powerful variable) differs from disturbance energy $\mathscr{E}+\mathscr{E}^0$ (see for instance Ripa 1992, §6).

3.1. *Basis for the vortex layer*

I shall discuss in some detail the eigensolutions of $-\mathrm{i}\mathbb{L}_{\mathrm{v}}\hat{\phi}_a = \hat{\omega}_a\hat{\phi}_a$, because this represents a physical problem of interest *per se*: the normal modes for the vortex in a $1\frac{1}{2}$-layer system (i.e. when the other layer is infinitely deep) and are closely related to the normal modes (from the state of rest) of Laplace tidal equations in a rotating paraboloid (see figure 3). The latter problem was solved by Miles & Ball (1963) from which the following results are easily obtained, adding the effects of the vortex swirl.

		$\hat{\omega}/f\,\mathrm{sgn}\,(m)$		
		$\epsilon \downarrow 0$	$\epsilon = \frac{1}{2}$	$\epsilon \downarrow 1$
Poincaré	$\mathscr{P}_n^{\pm}(n \geqslant 1)$	± 1	$\pm\frac{1}{2}(\hat{\kappa} \mp \lvert m\rvert)$	$\pm 1 - \lvert m\rvert$
Hybrid	$\mathscr{H}^{+}(n=0)$	0	$-\frac{1}{2}[\lvert m\rvert - (\lvert m\rvert)^{\frac{1}{2}}]$	$1 - \lvert m\rvert$
	$\mathscr{H}^{-}(n=0)$	-1	$-\frac{1}{2}[\lvert m\rvert + (\lvert m\rvert)^{\frac{1}{2}}]$	$-\lvert m\rvert$
Rossby	$\mathscr{R}_n(n \geqslant 1)$	0	$-\frac{1}{2}\lvert m\rvert$	$-\lvert m\rvert$

TABLE 2. Eigenvalue of the expansion components for the vortex layer (see figure 4)

Let $\hat{\phi} \equiv \exp(im\vartheta - i\hat{\omega}t)\,(\hat{P}(r),\, i\hat{U}(r),\, \hat{V}(r))^{\mathrm{T}}$, where I have omitted the subscript 'a' for simplicity, and the factor i is introduced so that the three functions of r can be chosen to be real. The two momentum equations are transformed into

$$(\hat{\omega}_*^2 - f_*^2)\,\hat{U} = f_*\, mr^{-1}\hat{P} - \hat{\omega}_*\,\hat{P}',$$
$$(\hat{\omega}_*^2 - f_*^2)\,\hat{V} = \hat{\omega}_*\, mr^{-1}\hat{P} - f_*\,\hat{P}',$$

where $f_* = f - 2\sigma$, $\hat{\omega}_* := \hat{\omega} + m\sigma$, and the prime indicates derivation with respect to r. Substitution into the continuity equation gives

$$r^{-1}(rg_{\mathrm{r}}H_{\mathrm{v}}\hat{P}')' + (\hat{\omega}_*^2 - f_*^2 + m\hat{\omega}_*^{-1}f_*\sigma(f-\sigma) - m^2r^{-2}g_{\mathrm{r}}H_{\mathrm{v}}\hat{P} = 0,$$

– recall that $g_{\mathrm{r}}H_{\mathrm{v}} = \frac{1}{2}\sigma(f-\sigma)\,(a^2 - r^2)$ – whose eigensolutions are of the form (Miles & Ball 1963)

$$\hat{P} \propto r^{|m|}\,{}_2F_1(-n,\, n+|m|+1;\, |m|+1;\, (r/a)^2),$$

where n is a non-negative integer and ${}_2F_1$ is an hypergeometric function (defined by ${}_2F_1(a, b; c; z) = 1 + abz/c1! + a(a+1)\,b(b+1)\,z^2/c(c+1)\,2! + \ldots$, which in this case becomes an nth degree polynomial; the dispersion relation is determined by

$$\hat{\omega}_*^2 + \mathrm{sgn}\,(m) f_*\,\hat{\omega}_* - |m|\sigma(f-\sigma) = 0 \quad \text{if } n = 0,$$

$$\frac{\hat{\omega}_*^2 - f_*^2}{\sigma(f-\sigma)} + m\frac{f_*}{\hat{\omega}_*} = \hat{\kappa}^2 \quad \text{if } n > 0,$$

where $\hat{\kappa}^2 := 2n(n+|m|+1)|m|$ (see figure 4).

For $n > 0$ there are three roots: two Poincaré waves, $\hat{\omega}_*^2 \approx f_*^2 + \hat{\kappa}^2\sigma(f-\sigma)$, and one (topographic) Rossby one, $\hat{\omega}_* \approx mf_*/[\hat{\kappa}^2 + f_*^2/(\sigma f - \sigma^2)]$. The former have high *intrinsic* frequency $\hat{\omega}_*$ (relative to the Coriolis parameter in the frame rotating with the basic vortex f_*); the latter has low intrinsic frequency. Notice that the type of component is not determined by the magnitude of the Doppler shifted frequency $\hat{\omega}$, relative the Coriolis parameter in the Earth's frame f.

For the gravest radial component, $n = 0$, the root $\hat{\omega}_* = \mathrm{sgn}\,(m) f_*$ is spurious and has been factored out. The remaining two components change continuously, as a function of ϵ, from being Poincaré-like in one extreme, to being Rossby-like in the other (very much like the Yanai waves do, in the equatorial β-plane); they will be called *hybrid* waves.

Poincaré and hybrid components are denoted by $\mathscr{P}_n^{\pm}$ and $\mathscr{H}^{\pm}$, where the sign is that of $\hat{\omega}_*/mf$, and Rossby ones by $\mathscr{R}_n$; see figure 4 and table 2.

Of course, in the related problem of Laplace tidal equations on a rotating paraboloid (Miles & Ball 1963), $\hat{\omega}_*$ and f_* in the above formulae are the actual frequency and Coriolis parameter, and there is total symmetry under the change $\epsilon \to 1 - \epsilon$. (In Miles' problem, ϵ does not have the meaning of a measure of vortex rotation; $\frac{1}{2}\epsilon(1-\epsilon)$, which is the square of the ratio between the deformation and domain radii, is the only important non-dimensional parameter.) In the problem of

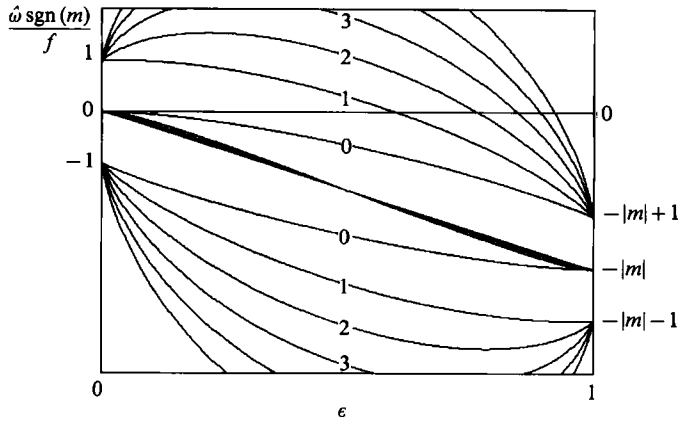

FIGURE 4. Eigenvalue of the expansion components for the vortex layer (see table 1); the label on the curves is the radial number n. The upper (lower) set of curves are the $\mathscr{P}_n^+$ ($\mathscr{P}_n^-$) Poincaré components ($n \geqslant 1$), and the set close to the Doppler shift $\hat{\omega} \approx -m\epsilon f$ are the Rossby components $\mathscr{R}_n$ ($n \geqslant 1$). Both hybrid components $\mathscr{H}^{\pm}$ ($n = 0$), change continuously from the Rossby set to one of the Poincaré sets. This figure in particular corresponds to $|m| = 3$, but it is quite generic; however, notice peculiarities of the $|m| = 1$ and $|m| = 2$ cases at the $\epsilon = 1$ end.

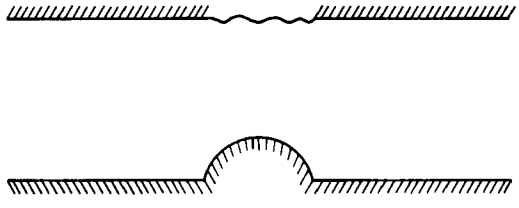

FIGURE 5. Equivalent physical system (cross-section) for the expansion components for the environment layer. Notice the difference to figure 1: the components are mathematical constructs, not (necessarily) physical waves.

this paper, on the other hand, this symmetry is lost, because of the Doppler shift $\hat{\omega} - \hat{\omega}_* \equiv -m\sigma$.

An interesting case is that of both hybrid waves ($n = 0$) for $m = \pm 1$: their frequencies are $\hat{\omega} = 0$, and $\hat{\omega} = \mp f$ (for all ϵ) and correspond to either a shift of the vortex centre or to the whole vortex performing inertial oscillations (as discussed by Nof 1991 in the case $\epsilon = \frac{1}{2}$), respectively.

3.2. *Basis for the environment layer*

Unlike the case of the previous section, the eigensolutions of $-\mathrm{i}\mathbb{L}_\epsilon \tilde{\phi}_b = \tilde{\omega}_b \mathbb{D}\tilde{\phi}_b$ do not correspond to a physically interesting case: they are mathematically equivalent to the free modes of a one-layer system with flat bottom and rigid lid for $r > a$, and with free surface and parabolic topography for $r < a$! (see figure 5). Certainly they are not the modes of the environment layer when the vortex layer is at rest: they are just a mathematical construct, useful for solving, and interpreting, the instability problem. This is the reason why I object to the use of the word *resonance*, which has physical implications, for the points $\hat{\omega} = \tilde{\omega}$.

Let $\tilde{\phi} \equiv \exp(\mathrm{i}m\vartheta - \mathrm{i}\tilde{\omega}t)(\tilde{P}(r),\ \mathrm{i}\tilde{U}(r),\ \tilde{V}(r))^{\mathrm{T}}$, the subscript '$b$' is omitted for simplicity. The two momentum equations of $-\mathrm{i}\mathbb{L}_\epsilon \tilde{\phi}_b = \tilde{\omega}_b \mathbb{D}\phi_\beta$ are transformed into

$$(\tilde{\omega}^2 - f^2)\,\tilde{U} = fmr^{-1}\tilde{P} - \tilde{\omega}\tilde{P}',$$
$$(\tilde{\omega}^2 - f^2)\,\tilde{V} = \tilde{\omega}mr^{-1}\tilde{P} - f\tilde{P}';$$

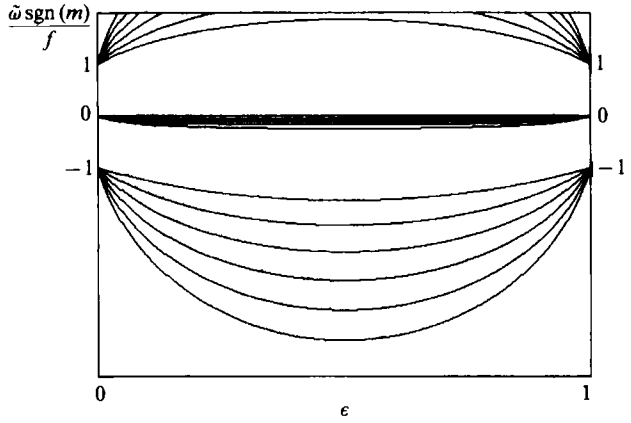

FIGURE 6. Eigenvalue of the expansion components for the environment layer. The upper (lower) set of curves are the $\mathscr{P}_n^+$ ($\mathscr{P}_n^-$) Poincaré components ($n \geqslant 0$), and the middle set are the Rossby components $\mathscr{R}_n (n \geqslant 0)$; there are no hybrid components in this case. This figure in particular corresponds to $|m| = 3$ and $\gamma = 0.9$, but it is quite generic; at smaller values of γ Poincaré (Rossby) components have larger (smaller) absolute frequencies.

		$\tilde{\omega}/f\,\mathrm{sgn}\,(m)$		
		$\epsilon \downarrow 0$	$\epsilon = \frac{1}{2}$	$\epsilon \downarrow 1$
Poincaré	$\mathscr{P}_n^{\pm} (n \geqslant 0)$	± 1	$\approx \pm \frac{1}{2}(\tilde{\kappa}^2+4)^{\frac{1}{2}}$	± 1
Rossby	$\mathscr{R}_n (n \geqslant 0)$	0	$\approx -\lvert m\rvert/(\tilde{\kappa}^2+4)$	0

TABLE 3. Eigenvalue of the expansion components for the environment layer (see figure 6)

substitution into the continuity equation gives $\tilde{P} \propto r^{-|m|}$ for $r > a$ (unless $\tilde{\omega} \equiv 0$) and

$$r^{-1}(r g_r H_e \tilde{P}')' + (\tilde{\omega}^2 - f^2 - m\tilde{\omega}^{-1} f\sigma(f-\sigma) - m^2 r^{-2} g_r H_e)\tilde{P} = 0,$$

for $r < a$, where it is $g_r H_e = \frac{1}{2}\sigma(f-\sigma)(a^2(\gamma^{-1}-1)+r^2)$. This equation must be solved subject to $\tilde{P} \sim r^{|m|}$ as $r \to 0$ and $\tilde{P}' = -|m| a^{-1} \tilde{P}$ at $r = a$ (see the Appendix for more details). The eigenvalues are given by

$$\frac{\tilde{\omega}^2 - f^2}{\sigma(f-\sigma)} - m\frac{f}{\tilde{\omega}} = \tilde{\kappa}^2(n, |m|, \gamma),$$

which, as before, has as solutions two Poincaré components, denoted by $\mathscr{P}_n^{\pm}$ (where the sign is that of $\tilde{\omega}_*/mf$), and a Rossby one, indicated by $\mathscr{R}_n$; see figure 6 and table 3. Notice that all dependence in ϵ (γ) is in the left- (right-)hand side of this equation. In the Appendix it is shown that $\tilde{\kappa}^2 > \frac{1}{2}(m^2+1) \geqslant |m|$ and therefore there are no roots with $\tilde{\omega}^2 = f^2$, like the spurious one for $n = 0$ in the vortex basis, which gave origin to the hybrid components.

4. Results

As explained in §3, I will start by considering instances of pairs of components, one from each layer, such that $\hat{\omega}_a = \tilde{\omega}_b$ in the wedge $(\hat{\omega}_a + m\sigma)\hat{\omega}_a < 0$, i.e. waves with opposite signs of pseudoenergy,

$$\hat{\omega}_a(\hat{\omega}_a + m\sigma)^{-1}|A_a|, \quad |B_b|^2,$$

Type of instability	Vortex mode	Environment mode	Azimuthal wavenumber	Restriction
Symmetric		NO	$m = 0$	
Baroclinic	$\mathscr{R}_n\, n \geqslant 1$	$\mathscr{R}_n\, n \geqslant 0$	$\lvert m\rvert \geqslant 1$	$2\epsilon < 1$
Hybrid	$\mathscr{H}^+\, n = 0$			
Sakai	$\mathscr{P}^+_n\, n \geqslant 1$	$\mathscr{R}_n\, n \geqslant 0$	$\lvert m\rvert \geqslant 2$	
Kelvin–Helmholtz	$\mathscr{H}^+\, n = 0$ $\mathscr{P}^+_n\, n \geqslant 1$	$\mathscr{P}^-_n\, n \geqslant 0$	$\lvert m\rvert \geqslant 3$	$2\gamma > \epsilon^{-1} - 1$

TABLE 4. Types of instability determined by pseudoenergy and angular pseudomomentum conservation (figure 2) and the dispersion relations of the basis components in each layer (figures 4 and 6). The hybrid type goes continuously from the baroclinic to the Sakai class.

and of angular pseudomomentum,

$$m(\hat{\omega}_a + m\sigma)^{-1}|A_a|^2, \quad m\tilde{\omega}_b^{-1}|B_b|^2.$$

From the results in figures 4 and 6, as well as tables 2 and 3, it follows that these 'resonances' occur in three main types of stability, summarized in table 4.

There are entries in table 4 for neither $m = 0$ (indeed normal modes symmetric or inertial instability was shown to be absent in this problem) nor for a perturbation which is Rossby-like in the vortex layer and Poincaré-like in the environment. This type of structure is not, of course, prohibited by pseudoenergy and angular pseudomomentum conservation; however, these laws would 'only' allow it to exist in the triangular-shaped region of figure 2: $\{(\epsilon, \gamma),\ 1 > \gamma > \frac{1}{2}(\epsilon^{-1} - 1)$ and $\frac{1}{3} > \epsilon > \frac{1}{2}\}$.

4.1. *Baroclinic instability*

This corresponds to a structure which is Rossby-like in both layers; pseudoenergy and angular pseudomomentum conservation predict that it cannot occur in the vertically hatched region of figure 2 ($\epsilon > \frac{1}{2}$; i.e. the region of the parameter space where the structure in the vortex layer is predicted to be Poincaré-like) and/or $m = 0$ (no wedge $(\hat{\omega}_a + m\sigma)\,\hat{\omega}_a < 0$).

Figure 7 shows the growth rate $\mathrm{Im}(\omega)$, as a function of (ϵ, γ), taking only the first Rossby component in each layer (for the scale of $\mathrm{Im}(\omega)$, see figure 8). The tongue of instability starts at $(\epsilon, \gamma) = (0^+, 0^+)$ (recall that for $\gamma \equiv 0$, and any ϵ, the vortex is stable) and widen for larger values of γ, all the way up to $\gamma = 1^-$. Notice that the instability region does not reach the $\epsilon > \frac{1}{2}$ region, where pseudoenergy and angular pseudomomentum conservation predict that the structure of a growing perturbation be Poincaré-like in the vortex layer (see figure 2).

The beginning of the instability tongue, at $\gamma \downarrow 0$, is determined as follows: if $\epsilon \to 0$ then $\hat{\omega} \sim -m\epsilon^2 f$; substituting in the dispersion relation for $\tilde{\omega}$ (chosen equal to $\hat{\omega}$), and recalling that $\tilde{\kappa}^2 \sim \frac{1}{2}j^2/\gamma$ as $\gamma \downarrow 0$ (where j is the $(n_e + 1)$th zero of the Bessel function of order $|m| - 1$; see the Appendix), it follows that

$$\gamma \sim \tfrac{1}{2}j^2(\hat{\kappa}^2 - 1)\,\epsilon^2 \quad \text{as } \epsilon \downarrow 0,$$

where $\hat{\kappa}^2 = 2n_v(n_v + |m| + 1) + |m|$ with $n_v \geqslant 1$ and $|m| \geqslant 1$. Moreover, looking at the normalization of the eigenfunctions in each layer (with the help of the integrals presented at the end of the Appendix) it is found $\hat{P}^2 = O(1)$ and $\tilde{P}^2 = O(\gamma/\epsilon)$, which

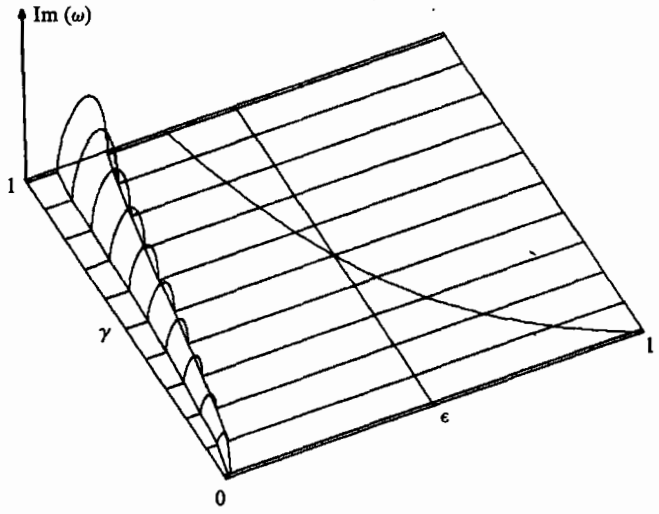

FIGURE 7. Growth rate as a function of (ϵ, γ), taking only two Rossby components: $\mathscr{R}_1$ in the vortex layer and $\mathscr{R}_0$ in the environment layer (baroclinic instability); the azimuthal wavenumber is equal to three. The boundaries of the regions of figure 2 are also drawn: notice that, for this type of instability, it is $\mathrm{Im}\,(\omega) \equiv 0$ where a growing perturbation in the vortex layer was predicted to be Poincaré-like.

yields $\mu^2 = O(\gamma/\epsilon) \equiv O(\epsilon)$; using this in the formula for ω calculated from two components with $\hat{\omega} = \tilde{\omega}$, it follows

$$\mathrm{Im}\,(\omega) = O(\gamma^{\frac{1}{2}}) = O(\epsilon) \quad \text{as } \gamma \downarrow 0.$$

The two-component calculation of figure 7 is complemented by that in figure 8, where the growth rate of all unstable modes found with 12×12 matrices $\mathbb{J}$ and $\mathbb{K}$, is plotted as a function of ϵ, for three values of $|m|$ and $\gamma = 0.9$. (I chose to show the results for a large value of γ, so that the differences between the 2×2 and 12×12 calculations stand out more clearly.) Several instability branches can be appreciated in this figure (particularly, closer to the $\epsilon = 0$ axis), but it is seen that one of them is well described by the simple 2×2 calculation (the addition of more degrees of freedom widens the stability region and increases the maximum growth rate, though, as expected).

4.2. *Sakai instability*

This corresponds to a structure which is Poincaré-like in the vortex layer and Rossby-like in the environment. Pseudoenergy and angular pseudomomentum conservation predict that it can only occur for $|m| \geqslant 2$, because otherwise there are no 'resonances' $\hat{\omega}_a = \tilde{\omega}_b$ in the wedge $(\hat{\omega}_a + m\sigma)\,\hat{\omega}_a < 0$ (see figures 4 and 6). This type of instability was first discovered by Sakai (1989), who called it Rossby–Kelvin instability, because the gravest Poincaré-like component in his case was a Kelvin wave. According to Sakai, this instability was also present in the (ageostrophic) calculation of Orlanski (1988).

Figure 9 shows the growth rate $\mathrm{Im}(\omega)$, as a function of (ϵ, γ), taking only one component in each layer: $\mathscr{P}^{+}_{1,\mathrm{v}}$ and $\mathscr{R}_{0,\mathrm{e}}$. The tongue of instability starts at $(\epsilon, \gamma) = (\epsilon_{\mathrm{c}}, 0^{+})$ and widens as γ increases. The critical Rossby number corresponds to the $\hat{\omega} \equiv 0$ crossing of the Poincaré component in the vortex layer (see figure 4), i.e. to $\hat{\omega}_{*} = m\epsilon_{\mathrm{c}} f$; substituting in the dispersion relation for the vortex components, it is found

$$\epsilon_{\mathrm{c}} \equiv (\hat{\kappa}^2 - 1)/(\hat{\kappa}^2 + m^2 - 2),$$

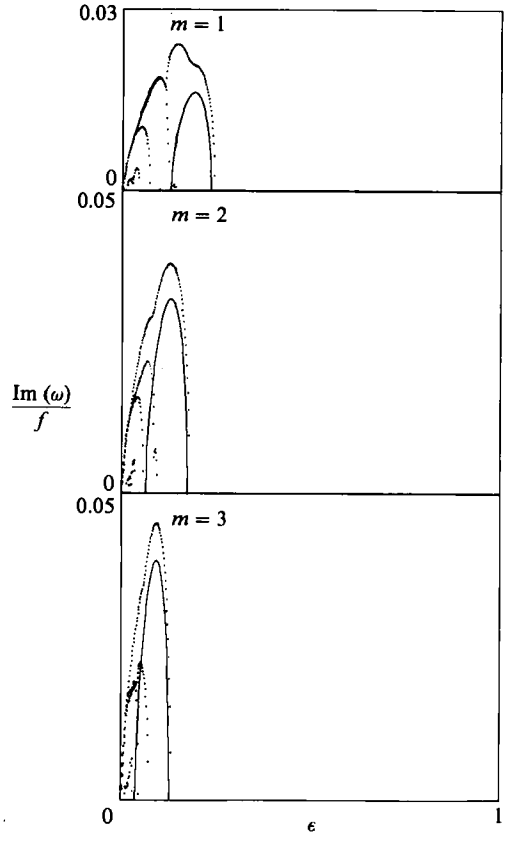

FIGURE 8. Growth rate as a function of ϵ, for the case of baroclinic instability. ——, two-component calculation of figure 7, ..., those obtained using twelve Rossby components: $\mathscr{R}_1 \ldots \mathscr{R}_6$ in the vortex layer and $\mathscr{R}_0 \ldots \mathscr{R}_5$ in the environment layer. $\gamma = 0.9$.

where $\hat{\kappa}^2 = 2n_v(n_v + |m| + 1) + |m|$, with $n_v \geqslant 1$and $|m| \geqslant 2$. Notice that, choosing n_v and $|m|$ appropriately, it is possible to find the beginning of an instability branch as close as desired to any value of ϵ. Close to the critical Rossby number it is easily found

$$\hat{\omega} \sim -\tau m f(\epsilon - \epsilon_c) \quad \text{as } \epsilon \downarrow \epsilon_c,$$

for some positive number τ; substituting in the dispersion relation for $\tilde{\omega}$ (chosen equal to $\hat{\omega}$), and recalling that $\tilde{\kappa}^2 \sim \frac{1}{2}j^2/\gamma$ as $\gamma \downarrow 0$, it follows that

$$\gamma \sim \tfrac{1}{2}j^2\tau(\epsilon - \epsilon_c) \quad \text{as } \epsilon \downarrow \epsilon_c,$$

where j is the $(n_e + 1)$th zero of the Bessel function of order $|m| - 1$. Looking, as before, at the normalization of the eigenfunctions in each layer, it is found $\hat{P}^2 = O(1)$ and $\tilde{P}^2 = O(\gamma)$, which yields $\mu^2 = O(\gamma)$; using this in the formula for ω calculated from two components with $\hat{\omega} = \tilde{\omega}$, it follows

$$\text{Im}\,(\omega) = O(\gamma) \quad \text{as } \gamma \downarrow 0.$$

The two-component calculation of figure 9 is complemented with that in figure 10, where the growth rate of all unstable modes found with 12×12 matrices $\mathbb{J}$ and $\mathbb{K}$, is plotted as a function of ϵ, for $\gamma = 0.9$ and two values of $|m|$ (there is no Sakai

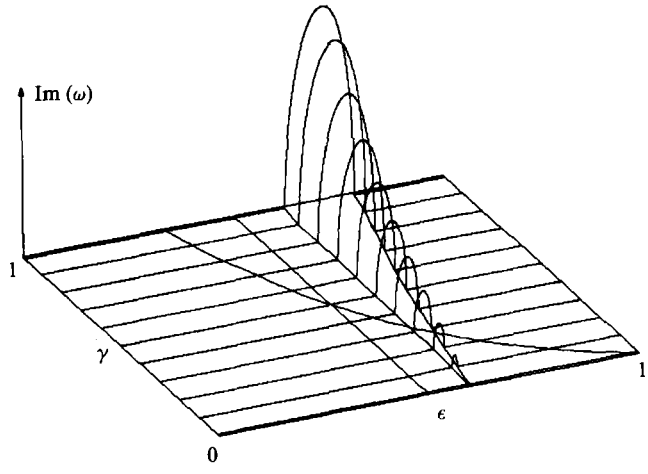

FIGURE 9. As in figure 7, for one Poincaré and one Rossby component $\mathscr{P}_1^+$ in the vortex layer and $\mathscr{R}_0$ in the environment layer (Sakai instability); $|m| = 3$. The instability region starts at $\epsilon = \frac{3}{5}^+$, $\gamma = 0^+$.

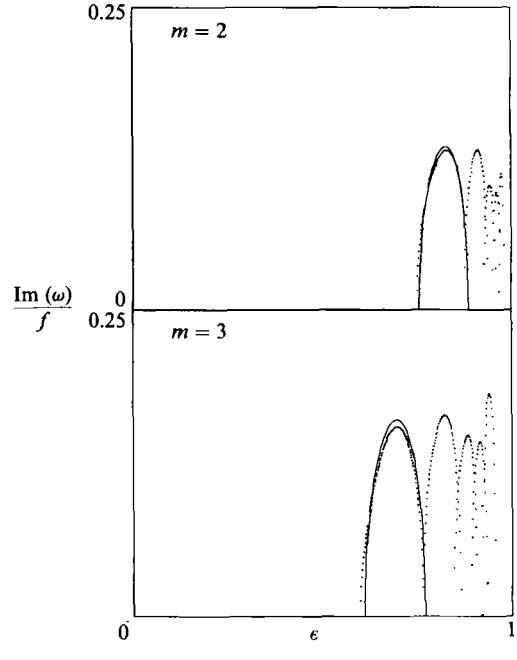

FIGURE 10. As in figure 8, for the case of Sakai instability. ——, two components of figure 9; ..., the following twelve components: $\mathscr{P}_1^+ \ldots \mathscr{P}_6^+$ in the vortex layer and $\mathscr{R}_0 \ldots \mathscr{R}_5$ in the environment layer. $\gamma = 0.9$.

instability for $|m| < 2$). Several instability branches can be seen in this figure (particularly, closer to the $\epsilon = 1$ axis), but it is clearly demonstrated that one of them is very well described by the simple 2×2 calculation of figure 9.

4.3. *Hybrid instability*

In the calculation of ω for the first two types, the hybrid component for the vortex layer was excluded on purpose. Figure 11 shows $\mathrm{Im}(\omega)$ as a function of (ϵ, γ), calculated using only $\mathscr{H}^+$ for the vortex layer and $\mathscr{R}_0$ for the environment layer. The

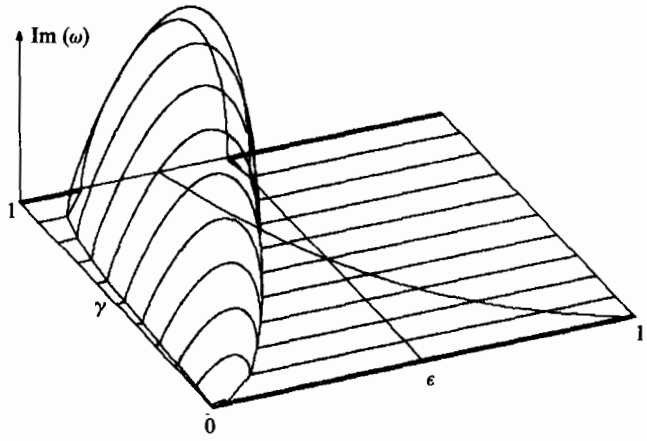

FIGURE 11. As in figure 7, for the hybrid component $\mathscr{H}^+$ in the vortex layer and the Rossby component $\mathscr{R}_0$ in the environment layer: this hybrid instability goes continuously from baroclinic instability (as in figures 7 and 8) at low Rossby numbers ϵ, to Sakai instability (as in figures 9 and 10) at larger values of ϵ.

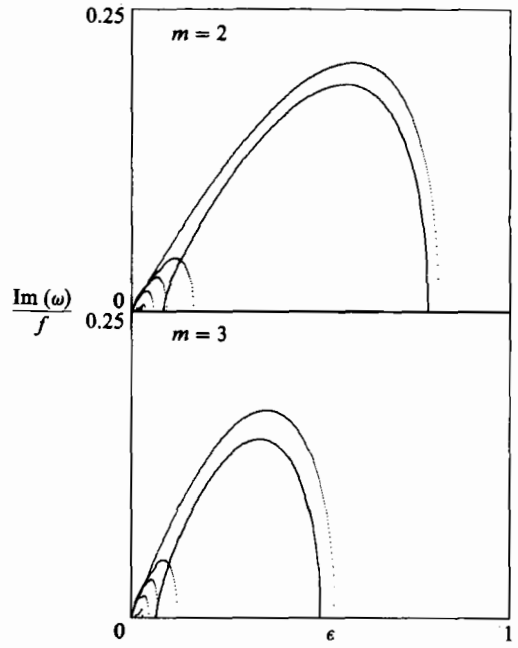

FIGURE 12. As in figure 8, for the case of hybrid instability: ——, the two components of figure 11, ..., the twelve components: $\mathscr{H}^+$, $\mathscr{R}_1 \ldots \mathscr{R}_6$ in the vortex layer and $\mathscr{R}_0 \ldots \mathscr{R}_5$ in the environment layer. $\gamma = 0.9$.

growth rate of all unstable modes found with 12×12 matrices $\mathbb{J}$ and $\mathbb{K}$, is presented in figure 12 as a function of ϵ, for $\gamma = 0.9$ and $|m| \geqslant 2$; there is no hybrid instability for smaller values of $|m|$ (recall comments on the hybrid components for $|m| = 1$, at the end of §3.1).

This branch has all the appearance of baroclinic instability, particularly near the origin $(\epsilon, \gamma) = (0^+, 0^+)$, where indeed it is well described by the analysis of §4.1, for $n_v = 0$ and $|m| \geqslant 2$. However, for larger values of γ (thicker eddies or shallower

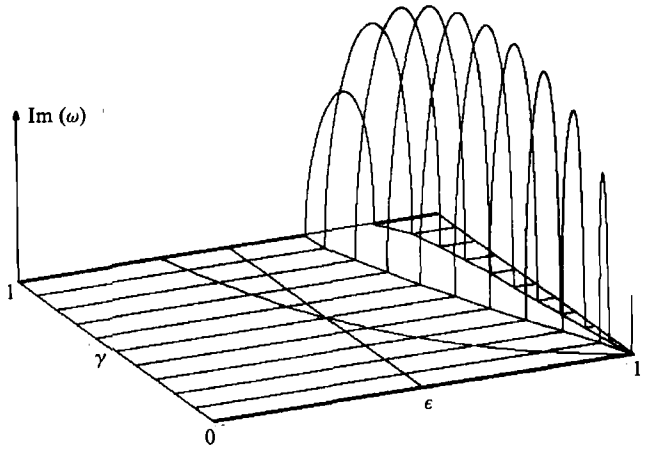

FIGURE 13. As in figure 7, for two Poincaré components: $\mathscr{H}^+$ in the vortex layer and $\mathscr{P}_0^-$ in the environment layer (Kelvin–Helmholtz instability); $|m| = 3$. Notice that, for this type of instability, $\mathrm{Im}\,(\omega) \equiv 0$ in the region of parameter space (figure 2) where the perturbation was predicted to be Rossby-like in the environment layer.

oceans) the instability region reaches the value $\epsilon = \frac{1}{2}$ (zero potential vorticity) here the hybrid component no longer behaves as a Rossby wave and it is rather a gravity one; recall that the effective Coriolis parameter is $f_* \equiv (1-2\epsilon)f$.

For instance for the $\mathscr{H}^+$ component it is

$$\frac{-\mathrm{i}H^2\hat{\xi}}{\boldsymbol{\nabla}\cdot(H\hat{\boldsymbol{u}})} = \frac{f_*}{\hat{\omega}_*} \equiv 2(1-2\epsilon)\,([4(|m|-1)\,\epsilon(1-\epsilon)+1]^{\frac{1}{2}}-1+2\epsilon))^{-1},$$

this expression diverges as $\epsilon \to 0$ (Rossby-like), vanishes for $\epsilon = \frac{1}{2}$ (Poincaré-like), and tends to -1 as $\epsilon \to 1$ (inertial oscillation); similarly the ratio of the two components of pseudomomentum is also given by $\mathscr{M} : \mathscr{C}_{\mathrm{M}} : : 2f_* : \hat{\omega}_*$. (For the $\mathscr{H}^-$ component, just change ϵ by $1-\epsilon$.) Consequently, this hybrid instability goes continuously from the Baroclinic type (for small ϵ) to the Sakai type (for large ϵ).

Paldor & Nof (1990) studied the problem of this paper for the particular case of $\epsilon = \frac{1}{2}$ (zero potential vorticity), and γ ranging from 1 to approximately 0.23. They found the eigenvalues ω by numerical integration of the coupled equations for p_{v} and p_{e}, and did not make a characterization of the associated perturbation structure. From the results of this paper, it is clear that what they found is the $\epsilon = \frac{1}{2}$ cross-section of the hybrid instability branches, which, at this value of ϵ, have the properties of a Sakai instability (see figures 11 and 12). It is interesting to notice that nothing special was found here at $\epsilon = \frac{1}{2}$, the growth rate curves pass continuously through that point.

4.4. *Kelvin–Helmholtz instability*

This classical type corresponds to a structure which is Poincaré-like in both layers. Pseudoenergy and angular pseudomomentum conservation predict that it can only occur for $|m| \geqslant 3$, because otherwise there are no 'resonances' $\hat{\omega}_a = \tilde{\omega}_b$ in the wedge $(\hat{\omega}_a + m\sigma)\,\hat{\omega}_a < 0$ (see figures 4 and 6). Moreover, this type of instability cannot happen for vortices in the horizontally hatched region of figure 2, where the structure of a growing perturbation was predicted to be Rossby-like in the environment layer.

Figure 13 shows the growth rate $\mathrm{Im}\,(\omega)$, as a function of (ϵ, γ), taking only one Poincaré component in each layer (in the vortex layer, $\mathscr{H}^+$ was used, which for these

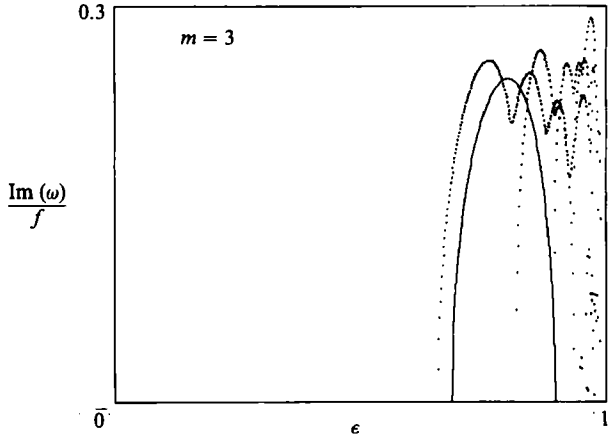

FIGURE 14. As in figure 8, for the case of Kelvin–Helmholtz instability. ——, the two components of figure 13, ..., the following twelve Poincaré components: $\mathscr{H}^+$, $\mathscr{P}_1^+ \ldots \mathscr{P}_5^+$ in the vortex layer and $\mathscr{P}_0^- \ldots \mathscr{P}_5^-$ in the environment layer. $\gamma = 0.9$.

large values of ϵ behaves as a Poincaré wave; see figure 4). The beginning of the instability tongue is at $(\epsilon, \gamma) = (1^-, 0^+)$; moreover, substituting $\tilde{\omega} \equiv \hat{\omega} = -f(m - \mathrm{sgn}\,(m))$ in the dispersion relation for the environment basis, and recalling that $\tilde{\kappa}^2 \sim \frac{1}{2}j^2/\gamma$ as $\gamma \downarrow 0$, it follows that

$$\gamma \sim \tfrac{1}{2}j^2(m^2 - |m|)\,(1-\epsilon) \quad \text{as } \epsilon \uparrow 1,$$

where j is the (n_e+1)th zero of the Bessel function of order $|m|-1$, and $|m| \geqslant 3$. Notice that this amply satisfies the requirement derived from pseudoenergy and angular pseudomomentum conservation (figure 2), which in this region reads $\gamma > \frac{1}{2}(1-\epsilon)$, as $\epsilon \uparrow 1$.

Finally, looking as before at the normalization of the eigenfunctions in each layer, it is found that $\hat{P}^2 = O(1-\epsilon) = O(\gamma)$ and $\tilde{P}^2 = O(1)$, which yields $\mu^2 = O(\gamma)$; using this in the formula for ω calculated from two components with $\hat{\omega} = \tilde{\omega}$, it follows

$$\mathrm{Im}\,(\omega) = O(\gamma^{\frac{1}{2}}) \quad \text{as } \gamma \downarrow 0.$$

The two-component calculation of figure 13 is complemented with that in figure 14, where the growth rate of all unstable modes found with 12×12 matrices $\mathbb{J}$ and $\mathbb{K}$, is plotted as a function of ϵ, for $\gamma = 0.9$ and $|m| = 3$ (there is no Kelvin–Helmholtz instability for smaller values of $|m|$). Several instability branches can be seen in this figure (particularly, closer to the $\epsilon = 1$ axis), but it is clearly demonstrated that one of them is quite well described by the simple 2×2 calculation of figure 13.

5. Summary

The stability of a solid-body rotating vortex in a two-layer system is studied in the whole extent of parameter space: $(\epsilon, \gamma) \in (0,1) \otimes (0,1)$, where ϵ, the Rossby number, is the ratio of the (anticyclonic) rotation rate to the Coriolis parameter, and γ^{-1} equals the model's total depth divided by the vortex maximum thickness. The pseudoenergy $\mathscr{I}_E$ and (angular) pseudomomentum $\mathscr{I}_M$ are the only integrals of motion, which are quadratic to lowest order in the perturbation; the following three results are derived from their conservation:

(*a*) There is no value of α such that $\mathscr{I}_E - \alpha \mathscr{I}_M$ is sight definite, for any pair of

parameters (ϵ, γ), i.e. no vortex in this class can be shown to be stable by Arnol'd's method.

(*b*) For an unstable vortex with $\epsilon > \frac{1}{2}$, an infinitesimal but growing perturbation must be Poincaré-like in the vortex layer, in the sense that it must have negative wave kinetic energy, and with a magnitude large enough to cancel the positive definite terms (wave kinetic energy in the environment layer, wave potential energy, and the 'wave Casimirs', whose integrands involve the square of the potential vorticity perturbation); Rossby waves have positive wave energy.

(*c*) Similarly, if $2\gamma < \epsilon^{-1} - 1$ (in particular, for any γ if $\epsilon < \frac{1}{3}$), a growing perturbation must be Rossby-like in the environment layer, in the sense that it must have negative wave Casimir, and with a magnitude large enough to balance the total wave energy and the wave Casimir in the vortex layer, which are positive definite in this region of parameter space (in a frame rotating with the vortex).

The normal mode equations are solved by means of a Galerkin expansion of the perturbation field (pressure and horizontal velocity) in each layer. Both bases are orthonormal and complete; moreover, each component has the distinct properties of a physical wave, Poincaré or Rossby, even though they are not a solution of the complete model equations *per se*. There are two members of the basis for the vortex layer, the hybrid components, which go continuously from being Rossby-like to being Poincaré-like, or vice versa, when ϵ varies from zero to unity.

Much insight on the nature of growing normal modes is gained with the greatest truncation of the expansion with non-trivial results: only two components, one from each layer. This strategy was pioneered by Sakai (1989) in the study of essentially the same problem, but in a channel, i.e. with linear, rather than azimuthal, symmetry. Instead of too-crude-an-approximation, this approach is a very useful one, because there are a myriad instability branches, which are well characterized, as summarized below, by this two-component calculation (whose results are later confirmed using more components of a similar type). Before going on with the description of the results, let me point out that, alas, this is not a universal method but, rather, its feasibility depends on the simplicity of the flow chosen for the basic state: uniform in each layer.

Pseudoenergy and (angular) pseudomomentum conservation imply that each one of the two components that build up a growing perturbation must have intrinsic frequencies of opposite signs in a frame rotating with the vortex and in the Earth's frame (i.e. that in which the environment is at rest for the basic solution). Use of this criterion with the eigenvalues of both bases allows for an *a priori* classification of the instability types, in the sense of their dynamical structure, as well as their possible values of ϵ, γ and azimuthal wavenumber m; this classification is *a posteriori* confirmed by the numerical analysis.

Three basic types of instability are found: baroclinic, Sakai, and Kelvin–Helmholtz; corresponding to a Rossby-like structure in both layers, Poincaré-like in the vortex layer and Rossby-like in the environment layer, and Poincaré-like in both layers, respectively. In addition, there is a hybrid type of instability (linked to the existence of the hybrid component in the vortex layer, which has the gravest radial dependence), which goes continuously from the baroclinic to the Sakai types, as ϵ grows away from zero. No instability type was found with a Rossby-like structure in the vortex layer and Poincaré-like in the environment layer: pseudoenergy and pseudomomentum conservation would 'only' allow this to exist in the triangular shaped region at the top of figure 2, which does not reach the $(\gamma = 0)$-axis.

All these instability types are realized in branches that emanate from a single point in the ($\gamma = 0$)-axis (environment infinitely deeper than the vortex) and widen up for finite values of γ. This is exemplified in figures 7, 9, 11 and 13, with the results of the two-component truncation for all (ϵ, γ), and compared in figures 8, 10, 12 and 14, with a twelve-component calculation made for a large value of γ, namely 0.9, in order to make the differences more clear.

Baroclinic instability branches start at $(\epsilon, \gamma) = (0^+, 0^+)$, with $\gamma = O(\epsilon^2)$ and a growth rate of $O(\gamma^{\frac{1}{2}})$; they never reach the ($\epsilon = \frac{1}{2}$)-line, as described by point (*b*) above. Hybrid instability branches start similarly (because they correspond to baroclinic instability for low γ) but do cross the ($\epsilon = \frac{1}{2}$)-line, where they correspond to a Sakai instability type. Baroclinic or hybrid instability require $|m| \geqslant 1$ or $|m| \geqslant 2$, respectively. Sakai instability branches start at $(\epsilon, \gamma) = (\epsilon_c, 0^+)$, where $0 < \epsilon_c < 1$, with $\gamma = O(\epsilon - \epsilon_c)$ and a growth rate of $O(\gamma)$. They are constrained by neither point (*b*) nor point (*c*) above, and require $|m| \geqslant 2$. Finally, Kelvin–Helmholtz instability branches start at $(\epsilon, \gamma) = (1^-, 0^+)$, with $\gamma = O(1-\epsilon)$ and a growth rate of $O(\gamma^{\frac{1}{2}})$. They never reach the $\gamma = (1-\epsilon)/2\epsilon$, as prescribed by point (*c*) above, and require $|m| \geqslant 3$. There is no symmetric (or inertial) instability, i.e. with a $m = 0$ perturbation, in this problem; not even for $\epsilon > \frac{1}{2}$.

Consequently, there are vortices unstable to perturbations with all azimuthal wavenumbers different from zero. In the $\frac{1}{2}$-layer case, on the other hand, elliptical vortices are unstable to infinitesimal perturbations with (the equivalent of) $|m| \geqslant 3$; however, at finite amplitudes one filament is formed, not three (Ripa & Jiménez 1988).

Sakai (1989) studied the ageostrophic version of Phillips' (1951) problem, i.e. an f-plane channel with uniform velocity in each one of two layers. This is the parallel counterpart of the basic flow in this work, rather than a system with uniform shear (e.g. Paldor & Killworth 1987). Sakai's analysis corresponds to approximately the ($\gamma = \frac{1}{2}$)-line in parameter space of this work, with ϵ roughly corresponding to $2F^2/(1+2F^2)$, where F is the Froude number in Sakai's paper. The three basic types of instability are present, in the same order, in Sakai's work; no hybrid instability is found, though, because there are no hybrid components available in his case.

Chassignet & Cushman-Roisin (1991) argue that the environment layer does not influence the vortex layer if (in the notation of this paper) $\gamma \ll \frac{1}{4}\epsilon^2(1-\epsilon)^2$. This criterion correctly excludes baroclinic and Kelvin–Helmholtz instabilities, which are the fastest – growth rate $O(\gamma^{\frac{1}{2}})$ – and are limited to $\gamma \geqslant O(\epsilon^2)$ as $\epsilon \downarrow 0$ and $\gamma \geqslant O(1-\epsilon)$ as $\epsilon \uparrow 1$, respectively. However, it does not exclude the slower Sakai instability – growth rate $O(\gamma)$ – which occurs at virtually any finite value of $\epsilon \in [0, 1]$.

The conclusion that the solid-body rotating vortices are unstable, in the two-layer model, does not mean that other swirl profiles can be stable or that similar structures may not be observed in more realistic systems, which might include forcing, dissipation and nonlinear effects (in particular, saturation of growing perturbations).

This work was supported by Mexico's Secretaría de Programación y Presupuesto, through CICESE's normal funding, and by the Consejo Nacional de Ciencia y Tecnología, under grant D111-903620. The heuristic arguments at the end of §2 were suggested by one of the reviewers.

Appendix

Changing the independent variable from r to $\rho := r/a$ and defining the parameter $\lambda^2 := \gamma^{-1} - 1$, the equation for $\tilde{P} = F(\rho)$ in $0 < \rho < 1$ takes the form

$$\rho^{-1}[\rho(\lambda^2+\rho^2)F']' + [2\tilde{\kappa}^2 - m^2 - m^2\lambda^2\rho^2]F = 0,$$
$$F \sim \rho^{|m|} \quad \text{as } \rho \to 0, \quad F'(1) = -|m|F(1),$$

where $\tilde{\kappa}^2$ is the eigenvalue. Unfortunately, I do not know of an analytic form for the eigensolutions of the environment components, except for $\lambda \to \infty (\gamma \to 0)$, which reduces the differential equation to that of Bessel functions. In this limit it is $\tilde{P} \sim J_\nu(j\rho)$ and $\tilde{\kappa}^2 \sim \frac{1}{2}j^2\lambda^2$, where $\nu = |m|$ and j is the $n+1$th zero of the Bessel function of order $\nu - 1$. Furthermore, writing the eigenvalue in the form

$$\tilde{\kappa}^2 := \tfrac{1}{2}j^2\lambda^2 + \tfrac{1}{2}\eta(\gamma),$$

ordinary perturbation theory yields

$$\tfrac{1}{2}\eta(0) = j^2 J_\nu^{-2}(j) \int_0^1 \mathrm{d}\rho\, J_\nu^2(j\rho)\rho^3 < \tfrac{1}{2}j^2.$$

In the other extreme, $\lambda \to 0$ $(\gamma \to 1)$, for $\rho \gg O(\lambda)$ it is $F \sim \rho^\nu$ with $(\nu+2) + 2\tilde{\kappa}^2 - m^2 = 0$, i.e. $F \sim \rho^{-1}\cos(\alpha + \beta \ln \rho)$, with $\beta^2 = 2\tilde{\kappa}^2 - m^2 - 1$; the boundary condition at $\rho = 1$ gives $\tan\alpha = (|m|-1)/\beta$. This solution must be matched with a inner function, valid for $\rho \leqslant \lambda$. Since the number of zero crossings between $\rho = 1$ and $\rho = O(\lambda)$ equals the radial mode number n, it must be $\alpha + \beta \ln \lambda \approx n\pi$, i.e.

$$\tilde{\kappa}^2 \sim \tfrac{1}{2}(m^2+1) + O\left(\frac{n\pi}{\ln\lambda}\right)^2 \quad \text{as } \lambda \to 0 \ (\gamma \to 1).$$

In sum, it is $\eta(1) = m^2 + 1$, and the convergence to this value is very slow.

For all finite values of γ, the differential equation was solved in the following way: first, the dependent variable is transformed to $G(\rho) := \rho^{-|m|}F(\rho)$; secondly, it is defined $H(\rho) := \partial G/\partial\tilde{\kappa}^2$; finally, G and H are calculated from the values $G = 1$, $G' = H = H' = 0$ at $\rho = 0$, and some initial guess of $\tilde{\kappa}^2$, all the way up to $\rho = 1$, using a fourth-order variable step Runge–Kutta integrator. The eigenvalue is then improved by Newton's method: $\tilde{\kappa}^2 \to \tilde{\kappa}^2 - (2|m|G + G')/(2|m|H + H')$. Of course, this algorithm needs a reasonably good initial guess: it was found that

$$\eta(\gamma) \approx (\eta(0) - m^2 - 1)(1-\gamma)^{\frac{1}{4}} + m^2 + 1$$

gives a good enough first estimate (convergence is achieved in a few iterations) in the whole interval $0 < \gamma < 1$ and for all values on n and m used.

In order to calculate the overlapping integral μ_{ab}, it is necessary to normalize the eigenfunctions of both bases so that $\langle \hat{\phi}_a, \hat{\phi}_a \rangle = [\tilde{\phi}_b, \tilde{\phi}_b] = 1$. For this purpose, it is not necessary to evaluate the velocity fields $\hat{\boldsymbol{u}}_a$ and $\tilde{\boldsymbol{u}}_b$ explicitly, because the following identities can be used:

$$\int_0^a g' H_\nu |\hat{\boldsymbol{u}}|^2 r\,\mathrm{d}r = \frac{2\hat{\omega}_*^2 - \sigma(f-\sigma)\hat{\kappa}^2}{\hat{\omega}_*^2 - f_*^2} \int_0^a |\hat{p}|^2 r\,\mathrm{d}r$$

$$\int_0^a [{}_2F_1(\ldots)\, r^{|m|}]^2 r\,\mathrm{d}r = \frac{(n!)^2 a^{2|m|+2}}{[(n+|m|)!\,|m|!]^2\,(4n+2|m|+2)},$$

for the vortex components, and

$$\int_0^\infty g' H_e |\tilde{\boldsymbol{u}}|^2 r \, \mathrm{d}r = \frac{2\tilde{\omega}^2 - \sigma(f-\sigma)\tilde{\kappa}^2}{\tilde{\omega}^2 - f^2} \int_0^a |\tilde{p}|^2 r \, \mathrm{d}r,$$

for the environment ones.

REFERENCES

Chassignet, E. P. & Cushman-Roisin, B. 1991 On the influence of lower-layer on the propagation of nonlinear ocean eddies. *J. Phys. Oceanogr.* **21**, 939–957.

Killworth, P. D. 1983 On the motion of isolated lenses on a beta-plane. *J. Phys. Oceanogr.* **13**, 368–376.

Miles, J. W. & Ball, F. K. 1963 On free-surface oscillations in a rotating paraboloid. *J. Fluid Mech.* **17**, 257–266.

Nof, D. 1991 Orbiting eddies. *Tellus* **43**, 64–67.

Orlanski, I. 1968 Instability of frontal waves. *J. Atmos. Sci.* **25**, 178–200.

Paldor, N. & Killworth, P. D. 1987 Instabilities of a two-layer coupled front. *Deep Sea Res.* **34**, 1525–1539.

Paldor, N. & Nof, D. 1990 Linear instability of an anticyclonic vortex in a two-layer ocean. *J. Geophys. Res.* **95**, 18,075–18,079.

Phillips, N. A. 1951 A simple three-dimensional model for the study of large-scale extratropical flow patterns. *J. Atmos. Sci.* **8**, 381–394.

Ripa, P. 1982 Nonlinear wave–wave interactions in a one-layer reduced gravity model on the equatorial beta-plane. *J. Phys. Oceanogr.* **12**, 97–111.

Ripa, P. 1987 On the stability of elliptical vortex solution of the shallow-water equations. *J. Fluid Mech.* **183**, 343–363.

Ripa, P. 1991 General stability conditions for a multi-layer model. *J. Fluid Mech.* **222**, 119–137.

Ripa, P. 1992 Wave energy-momentum and pseudo energy-momentum conservation for the layered quasi-geostrophic problem. *J. Fluid Mech.* **235**, 379–398.

Ripa, P. & Jiménez, S. 1988 Evolution of an unstable elongated eddy. *J. Phys. Oceanogr.* **18**, 1202–1205.

Sakai, S. 1989 Rossby–Kelvin instability: a new type of ageostrophic instability caused by a resonance between Rossby waves and gravity waves. *J. Fluid Mech.* **202**, 149–176.

Takehiro, S. I. & Hayashi, Y. Y. 1992 Over-reflection and shear instability in a shallow water model. *J. Fluid Mech.* **236**, 259–279.